Fluorescence line narrowing spectral studies of Eu³⁺-doped lead borate glass

V. Venkatramu [a], D. Navarro-Urrios [b,1], P. Babu [a,c], C.K. Jayasankar [a,*], V. Lavín [b]

[a] *Department of Physics, Sri Venkateswara University, Tirupati 517 502, India*
[b] *Departamento de Física Fundamental y Experimental, Electrónica y Sistemas, Universidad de La Laguna, E-38200 La Laguna, Tenerife, Spain*
[c] *Department of Physics, Government College for Men, Wanaparthy 509 103, India*

Abstract

A lead borate glass of molar composition 49.5H$_3$BO$_3$–49.5PbO–1.0Eu$_2$O$_3$ was prepared and studied by broadband and fluorescence line narrowing spectral techniques. Site-selective $^5D_0 \rightarrow {}^7F_{0,1}$ emission spectra were obtained under resonant excitation at different wavelengths along the $^7F_0 \rightarrow {}^5D_0$ transition. These studies have been used to investigate the site-to-site variations in the spectroscopic properties of Eu^{3+} ions in the lead borate glass at 13 K. The energies of the Stark levels of the $^7F_1$ multiplets are obtained from the experimental fluorescence line narrowing spectra and crystal-field analysis has been carried out, assuming C$_{2v}$ orthorhombic symmetry, for each of the excitation energies. The distribution environments and the local structures of Eu^{3+} ions in lead borate glass are found to be almost similar to calcium diborate glass and lies intermediate between Eu^{3+}-doped sodium borosilicate and lithium fluoroborate glasses.
© 2005 Elsevier B.V. All rights reserved.

1. Introduction

Lanthanide ion-doped glasses are used nowadays as an extremely important class of optical devices such as lasers, fiber amplifiers, light converters, sensors and hole burning high-density memories [1,2]. The optical spectrum of a lanthanide ion is closely related to the particular local symmetry of the environment occupied by this ion in solid matrices. In glasses, they usually consist in inhomogeneously broadened bands due to site-to-site variations in the local field acting on the ions [3].

Applying the fluorescence line narrowing (FLN) technique it is possible to excite selectively the optically active ions in a particular environment by tuning the wavelength of a laser light within an absorption band [4–7]. This technique has become the most powerful experimental tool for the study of local structural inhomogeneties of rare earth ions in glasses. Moreover, Eu^{3+} is the most suitable ion for FLN studies in glasses because of its unique energy level structure with non-degenerate ground ($^7F_0$) and excited ($^5D_0$) states and the fact that its luminescence shows a high dependence with the environment. As the excited state, $^5D_0$, is a singlet, the structure in the fluorescence spectra is determined solely by the terminal-level splitting, which is in turn related to local symmetry around the Eu^{3+} ion.

Binary lead borate glasses xPbO–B$_2$O$_3$ form an interesting glass system because the glass phase can be

* Corresponding author. Tel.: +91 877 2249666; fax: +91 877 2225211.
E-mail address: ckjaya@yahoo.com (C.K. Jayasankar).
[1] Present address: INFM and Dipartimento di Fisica, Università degli Studi di Trento, Via Sommarive 14, Povo, 38050 Trento, Italy.

obtained over a wide concentration range of lead oxide [8]. The lead oxide acts as a modifier of borate glasses at low concentration ($x < 0.2$) and becomes also a glass former at higher concentration [9]. The structure of the borate glass is a random 3-D network builded by different borate groups formed by the gathering of BO_3 and BO_4 units [10]. Moreover, the concentration of the modifier ion plays a relevant role in the presence of different groups.

This work presents a detailed study of influence of the local structure in the optical properties of Eu^{3+} ion in lead borate glass of composition (in mol%) $49.5H_3BO_3$–$49.5PbO$–$1.0Eu_2O_3$. Broadband excitation and luminescence at RT and FLN spectra at 13 K, in the excitation range of 577–581 nm within the inhomogeneous absorption band of $^5D_0 \rightarrow {}^7F_0$, are used to analyze the distribution of local structures and the strength of the crystal-field around the Eu^{3+} ion in lead borate glass. Results are compared with some of the reported Eu^{3+}-doped glasses.

2. Experimental

The Eu^{3+}-doped lead borate glass with the composition (in mol%) of $49.5H_3BO_3$, $49.5PbO$ and $1.0Eu_2O_3$ was prepared by melt quenching technique [5]. Broadband excitation spectra were obtained by exciting the sample with light from a 250 W halogen lamp passed through a 0.25 m single-grating monochromator. For FLN measurements, a tunable dye laser operating with Rhodamine 6G, pumped by Q-switched 532 nm frequency-doubled Nd:YAG laser, was used. Fluorescence was recorded using a 0.25 m double-grating monochromator with a cooled photomultiplier using a photon counting technique. Decay curves were obtained using a digital storage oscilloscope interfaced to a personal computer. For measurements at 13 K, the sample was cooled in a helium closed-cycle cryostat.

3. Results

Excitation and emission spectra of the Eu^{3+} ions in a lead borate glass doped with 1 mol% of Eu_2O_3, obtained under broadband excitation at RT, are given in Fig. 1. Partial free-ion energy level scheme for Eu^{3+} ion is also shown in Fig. 1. Electronic and vibronic excitation spectra associated to the $^7F_0 \rightarrow {}^5D_0$, $^5D_2$ transitions observed at 13 K are shown in Fig. 2. Phonon side bands (PSB) associated to pure electronic bands (PEB) ($^7F_0 \rightarrow {}^5D_0$ and $^7F_0 \rightarrow {}^5D_2$) are shown in Fig. 2. The PSB, due to compositional changes of Li_2O and PbO associated to $^7F_0 \rightarrow {}^5D_2$ are compared in Fig. 2. The lifetimes determined for $^5D_0$ level at different excitation wavelengths are also shown in Fig. 2.
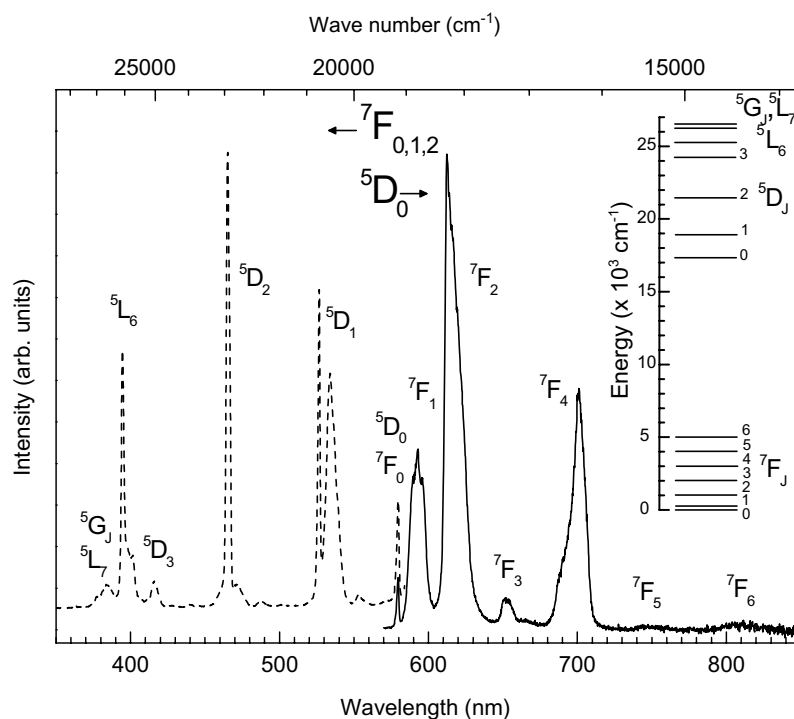

Fig. 1. Broadband excitation (---) and emission (—) spectra of a lead borate glass doped with 1 mol% of Eu_2O_3 at RT. Transitions start from the $^7F_0$ and the thermalized $^7F_1$ and $^7F_2$ levels in the excitation spectrum, detecting the $^5D_0 \rightarrow {}^7F_2$ transition at 612 nm, and from the $^5D_0$ level in the emission one, exciting the $^7F_0 \rightarrow {}^5L_6$ transition at 395 nm. Partial energy level diagram of the free Eu^{3+} ion is also shown.
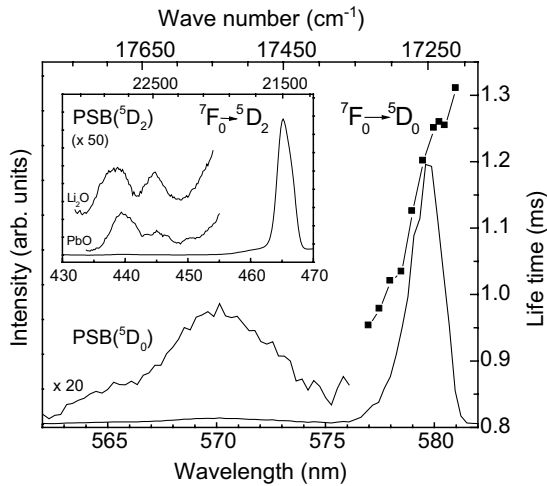
Fig. 2. Electronic and vibronic excitation spectra associated to the $^7F_0 \rightarrow {}^5D_0$ and $^7F_0 \rightarrow {}^5D_2$ transitions monitoring the $^5D_0 \rightarrow {}^7F_2$ transition at 612 nm in a lead borate glass doped with 1 mol% of Eu_2O_3 at 13 K. Lifetime of the $^5D_0$ level as a function of the excitation wavelength is also shown.

The FLN emission spectra of the $^5D_0 \rightarrow {}^7F_1$ transition at 13 K, obtained by laser excitation at different wavelengths along the electronic $^7F_0 \rightarrow {}^5D_0$ absorption band are shown in Fig. 3. Fig. 4 shows the scalar crystal field strength $N_v(B_{2q})$ versus maximum splitting observed for the $^7F_1$ level. The values of $N_v(B_{2q})$ have been determined from the $^7F_1$ Stark levels by considering both for with and with out J-mixing following the procedure described in Refs. [5,6,11,12]. The $^7F_1$ Stark levels with respect to $^7F_0$ level as a function of the excitation wavelength are also shown in the inset of Fig. 4. Scalar crystal–field strength $N_v(B_{2q})$, with J-mixing, versus excitation wavelength to the $^5D_0$ level for lead borate glass is compared with other Eu^{3+} doped glasses in Fig. 5 [5,6,13].

4. Discussion

Fig. 1 shows the excitation and emission spectra of the Eu^{3+} ions doped in a lead borate glass. They consist a set of inhomogeneously broadened bands, each one associated to a transition between different $^{2s+1}L_J$ multiplets within the $4f^6$ ground configuration. They start from the low emitting level $^5D_0$ for the emission spectrum, whereas the ground $^7F_0$ and the thermalized $^7F_1$ and $^7F_2$ are the initial levels for the excitation one. The intraconfigurational $4f^6$–$4f^6$ transitions of the Eu^{3+} ions were identified comparing the peak energies with the free Eu^{3+} ion energy level diagram (see Fig. 1) [14].

The most interesting feature is the absence of emission starting from any level above the lowest emitting level, i.e. the $^5D_0$ level, that can be ascribed to the existence of high energy phonons in borate glasses
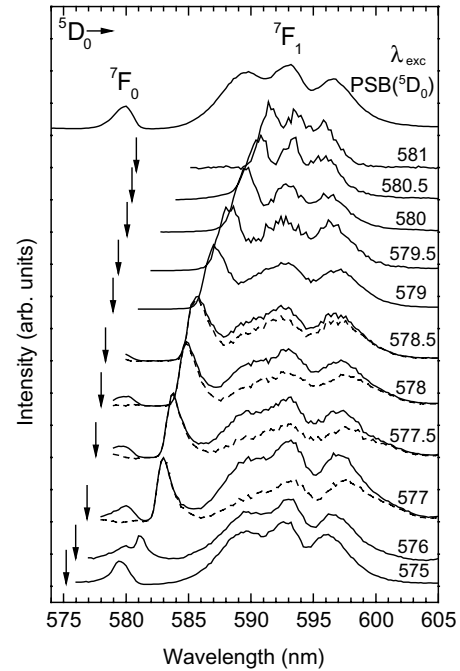

Fig. 3. FLN emission spectra to the $^7F_1$ stark levels exciting selectively within the $^7F_0 \rightarrow {}^5D_0$ electronic absorption band in a lead borate glass doped with 1 mol% of Eu_2O_3 at 13 K. Spectra are normalized to the maximum of the high-energy peak of the $^7F_0 \rightarrow {}^5D_1$ transition. The excitation wavelengths are shown on the right side of each trace in nm and with vertical arrows. The upper spectrum is the broadband emission to the $^7F_{0,1}$ levels obtained by exciting the PSB coupled to the $^5D_0$ level at 13 K. Dotted lines indicate the spectra obtained after subtracting the broadband contribution.
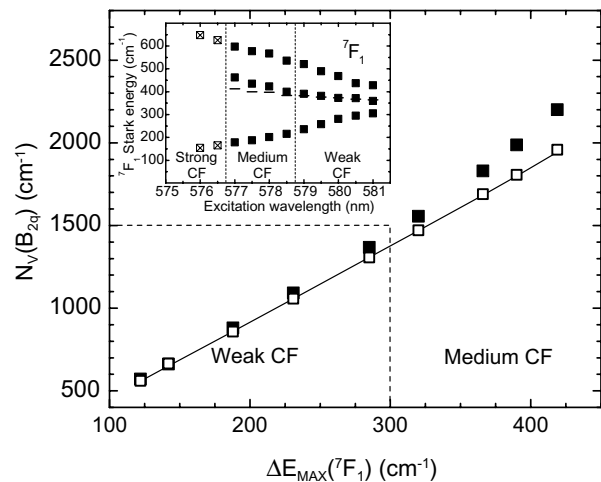

Fig. 4. Scalar crystal-field strength $N_v(B_{2q})$, with (■) and without (□) taking into account the ‘J-mixing’, as a function of the maximum splitting observed for the $^7F_1$ level of the Eu^{3+} ions in a lead borate glass. The solid line indicates the fit to the theoretical expression of Malta et al. [12]. The inset shows the positions of the $^7F_1$ Stark levels with respect to the $^7F_0$ level as a function of the excitation wavelength. Dashed line indicates barycenter of the $^7F_1$ level.

($>1000 \, cm^{-1}$). Thus, after exciting the $^7F_0 \rightarrow {}^5L_6$ transition at 395 nm, broadband emission spectrum consists
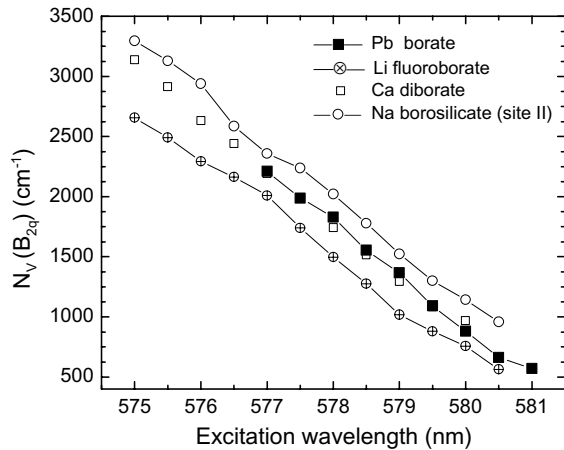
Fig. 5. Scalar crystal-field strength $N_v(B_{2q})$, with 'J-mixing', as a function of the excitation wavelength to the $^5D_0$ level for lead borate, lithium fluoroborate [5], calcium diborate [6] and sodium borosilicate [13] glasses.

of different bands associated to the $^5D_0 \rightarrow ^7F_J$ ($J = 0$–6) transitions. The $^5D_0 \rightarrow ^7F_1$ transition is magnetic dipole in nature and is allowed by all selection rules and its line strength is almost site independent [6]. Since the initial emitting level is non-degenerated, the existence of three overlapped peaks for this transition indicates low symmetry (orthorhombic, triclinic or monoclinic) of the Eu^{3+} ion environments in this glass. The $^5D_0 \rightarrow ^7F_J$ ($J = 2, 4, 6$) transitions are electric dipole in nature and are forced by the odd CF Hamiltonian. The other emission transitions $^5D_0 \rightarrow ^7F_J$ ($J = 0, 3, 5$) are strictly forbidden and their low intensities are due to J-mixing effect between multiplets [15]. The ratio of the intensities of the $^5D_0 \rightarrow ^7F_2$ and the $^5D_0 \rightarrow ^7F_1$ transitions gives a measure of the degree of distortion from inversion symmetry of the local environment of the Eu^{3+} ion in glasses [5]. The value of R in lead borate glass is found to be 2.9, which lies within the range of values (2–7) found in oxide glasses [16], but it is significantly lower than 3.5 found in lithium borate glasses. This low value of R indicates that the Eu^{3+} ions in lead borate glass occupy relatively low-symmetry sites.

As seen from Fig. 2, the existence of $^7F_0 \leftrightarrow ^5D_0$ transitions is due to the J-mixing effect, otherwise they are forbidden by selection rules. For orthorhombic and higher symmetries the 'second rank crystal-field' felt by the Eu^{3+} ions is described in the Wybourne's notation by the Hamiltonian [17,18],

$$H_{CF} = B_{20}C_0^{(2)} + B_{22}(C_{-2}^{(2)} + C_2^{(2)}), \qquad (1)$$

where B_{20} and B_{22} are the CF parameters. Thus the second rank even CF Hamiltonian allows mixing of wave-functions from the $^7F_2$ Stark levels ($J = 2$, $M = 0, \pm2$) with that of $^7F_0$ level ($J = 0$, $M = 0$). Moreover, the inhomogeneous broadening of the $^7F_0 \rightarrow ^5D_0$ transition is a consequence of overlapping of the homogeneous

bands associated to Eu^{3+} ions in different environments. This electronic band has no internal structure and its inhomogeneous linewidth gives a direct measure of the energy distribution of the different Eu^{3+} sites. It is worth noting that the full width at half maximum (FWHM) of the $^7F_0 \rightarrow ^5D_0$ transition for the lead borate glass is 55 cm^{-1} and is just slightly higher than 50 cm^{-1} found in fluorozirconate glass [4] and appreciably lower than 65 and 80 cm^{-1} found in lithium fluoroborate and borate glasses, respectively [5]. This relatively small width of the inhomogeneous band is the evidence of the narrow distribution of environments for the Eu^{3+} ions in lead borate glass compared with other pure oxide borate glasses, being similar to that found in fluoride glasses.

Moreover, it suggests the presence of a high concentration of non-bridging oxygens around the Eu^{3+} ion [19]. This is consistent with the nuclear magnetic resonance (NMR) studies [20,21], which indicates that at higher PbO concentration (>20 mol%), Pb acts as a glass former with progressively more covalent bonding. As the PbO_4 units bridge preferentially to BO_3^- rather than to BO_4^- units, the number of non-bridging oxygens increases.

Apart from the intraconfigurational $4f^6$–$4f^6$ transitions, known as zero-phonon or PEB, the coupling of the f-electrons with the ligands gives rise to simultaneous transitions between electronic states of the Eu^{3+} ion and the vibrational states of the dopant host system. The latter gives rise to vibronic or PSB involving the internal vibrations of the structural groups forming the immediate environment of the Eu^{3+} ions. Taking into account the rather low probability of multiphonon excitation, the difference in energy between the PSB and the PEB corresponds to the energy of one phonon [22]. As can be seen in Fig. 2, a PSB is observed with a maximum at an energy of around 290 cm^{-1} and a small band at around 450 cm^{-1} above the $^7F_0 \rightarrow ^5D_0$ PEB. Moreover, three main bands are observed in the PSB associated to the $^7F_0 \rightarrow ^5D_2$ transition (see Fig. 2) at around 700, 960 and 1250 cm^{-1} above the PEB.

Due to the disordered nature of the vitreous materials and the great numbers of possible borate groups, the interpretation of the vibronic spectra is not an easy task. However, the PSB associated to the $^7F_0 \rightarrow ^5D_0$ transition linked to low-energy phonons up to 500 cm^{-1} is known to be due to Eu–O stretching vibrations [23–25]. This fact and the relatively well defined structure of this PSB compared to other borate matrices [5] seems to be related to the presence of heavy ions like Pb in the Eu–O bonds of the optically active ions local structure in the lead borate glass. On the other hand, it is generally accepted that those bands associated to high-energy phonons are due to vibrations of the structural groups involving light ions like boron. Thus those PSB in the range from 1100 to 1500 cm^{-1} corresponds to borate groups containing BO_3 units, while for lower energies

are associated to groups containing BO_4 tetrahedra (880–1050 cm^{-1}) and to the B–O–B bonds (690–770 cm^{-1}) [10,26], all of them in the immediate environment of the Eu^{3+} ion. It is worth noting that the relatively large PSB peak at 1250 cm^{-1} compared with the other two which indicates the presence of greater number of BO_3 units forming tetraborate groups (associations of triborate and pentaborate groups) [26] in the local structure of the Eu^{3+} ions.

The above hypothesis has been supported by the NMR [20,21] and Raman spectroscopy studies [27], wherein the larger concentration of PbO (>30 mol%) caused decrease in the BO_4 units and generating a high concentration of non-bridging oxygens around the Eu^{3+} ion. Moreover, it is quite interesting comparing with the PSB measured in lithium borate glasses with the same compositional percentage (see Fig. 2). Apart from the fact that there are more and stronger bands associated to BO_3 and BO_4 units in the lithium borate glass, there is also a strong band centered at around 1250 cm^{-1}. Its presence has been related with the breakdown of the rigidity of the diborate groups by the Li^+ ions, destroying the intradiborate bond between the tetrahedrically coordinated pair of borons, and strongly polarizing or taking the bridge-oxygen used to connect them [28]. This process gives rise to a larger B–O overlapping of the BO_3 units, although the tetrahedrical character of the bond is kept by connecting with other boron ions through interdiborate bridges. This open system allows distortions necessary for the Li^+ ion to coordinate with a low number of oxygens and at shorter distances. This result is in accordance with the hypothesis of Bray et al. [20] suggesting that lead ions enter, in this concentration, not only as modifiers but also as a glass network in the form of PbO_4 pyramid units that are preferentially bridged to BO_3 units rather than to BO_4 ones. Thus the flexibility shown in lithium borate glasses is assumed to exist also in the lead borate glass, in such a way that the Eu^{3+} ions occupy more ordered and closer in energy environments.

FLN emission spectra to the $^7F_1$ Stark levels exciting selectively with in the $^7F_0 \rightarrow {}^5D_0$ electronic absorption band in Eu^{3+} doped lead borate glass at 13 K are shown in Fig. 3. The line narrowing effect is clearly visible, particularly for the high-energy component that shifts linearly with the excitation wavelength, and is attributed to the progressive increase in the magnitude of the local crystal-field acting on the Eu^{3+} ions.

For excitation wavelengths above 579 nm, the transition presents the expected three peaks due to the complete removal of the degeneracy of the $^7F_1$ level by the crystal-field. For lower excitation wavelengths from 578.5 to 577 nm, the low energy components undergo progressive broadening and generate some extra peaks in the emission spectra. In the emission profile obtained at an excitation of 576 nm, the high-energy component

overlaps with the $^5D_0 \rightarrow {}^7F_0$ transition while the rest of the spectrum is similar to the inhomogeneous one obtained by exciting any level above the $^5D_0$ level. For excitation at 575 nm the emission spectrum is practically the same as the inhomogeneous spectrum. A complete lose of selectivity is also found for the emission band exciting within the PSB coupled to the $^5D_0$ level, i.e. the spectrum obtained is always the same and identical to the inhomogeneous one.

This loss of selectivity in the laser excitation is due to the overlapping of the high-energy side of the PEB with the tail of the PSB of the $^5D_0$ level (Fig. 2) and the feature that the PSB is common to all the Eu^{3+} ions in all the environments possible in the glass. Another possible explanation is related to the presence of two main sites for the optical active ions in the glass. Thus the $^5D_0 \rightarrow {}^7F_1$ emission profile would be due to the simultaneous excitation of Eu^{3+} ions in these two sites [5], to energy transfer processes between them [6,29] or to the combination of both mechanisms [30]. Although the presence of two main sites is not clear, evidences of energy migration between Eu^{3+} ions in environments close in energy but spectrally different [29] can be experimentally observed as a band in the $^5D_0 \rightarrow {}^7F_0$ region for excitation wavelength from 575 to 578.5 nm. In any case, in order to determine as exactly as possible the positions and relative intensities of the $^5D_0 \rightarrow {}^7F_1$ low-energy components of the Eu^{3+} ions selectively excited, the inhomogeneous contribution have been subtracted [4,5] and the spectra obtained are shown in dotted lines in Fig. 3.

The distribution of environments in lead borate glass is also evident from the decay curves, which are single exponential, and the lifetimes that are found to increase with the excitation wavelength as can be seen in Fig. 2. The site-selective temporal evolution of the $^5D_0$ luminescence was detected monitoring the high-energy Stark component of the $^5D_0 \rightarrow {}^7F_1$ emission. Lifetime decreases with crystal-field (CF) strength around the Eu^{3+} ions due to the increase in the non-radiative migration of energy between the Eu^{3+} ions, as multiphonon relaxation is negligible for the $^5D_0$ level, and to structural changes in the local structure.

As a conclusion, the systematic variations observed in the energy positions, the lifetimes and the presence of the inhomogeneous contribution from all the optical active ions from simultaneous excitation allow us to assume the existence of a unique kind of site for all the environments for the Eu^{3+} ions in the lead borate glass.

The CF strength experienced by the Eu^{3+} ions is a measure of their electrostatic interaction with the surrounding oxygens. A higher CF strength is due to larger charge density and/or to a smaller Eu–O distance. The average strength of the crystal-field acting on the Eu^{3+} ions in lead borate glass can be estimated from the splitting of the $^7F_1$ multiplets in to three Stark components.

From the FLN measurements, positions of the $^7F_1$ Stark levels with respect to $^7F_0$ ground level are collected and plotted as a function of excitation wavelength in Fig. 4 (inset). The dashed line indicates the barycenter of the $^7F_1$ level, which shifts to higher energies with the excitation energy. As already mentioned, the change in the energy positions of the $^7F_1$ Stark levels with excitation energy is attributed to the progressive increase in the magnitude of the local crystal-field acting on the Eu^{3+} ion. The central $^7F_1$ Stark level deviates marginally with respect to the barycenter where as low and high energy Stark levels vary largely with increase in excitation energy. Similar behavior has been observed for Eu^{3+}-doped lead germanate glasses [7]. The crossed squares have been obtained taking into account only the high-energy peak exciting at 576 nm and using an extrapolation of the $^7F_1$ Stark energy positions.

Since the splitting of the $^7F_1$ multiplet is only due to the second rank even crystal-field, the B_{20} and B_{22} CF parameters have been calculated by diagonalizing the complete Hamiltonian (free-ion Eu^{3+} plus the second rank CF) using C_{2v} symmetry, which is the highest orthorhombic symmetry that allows full splitting of $^7F_1$ levels of the Eu^{3+} ion. Calculations include both those taking into account and those not taken into account the J-mixing effect between the 49 ^7F_J ($J = 0$–6) Stark levels. Moreover, the scalar crystal-field strength parameter N_v [11,12], that relates the CF strength with the maximum splitting of the $^{2s+1}L_J$ levels, has been also calculated considering only the second rank CF parameters, and is given by

$$N_v(B_{2q}) = \sqrt{\frac{4\pi(B_{20}^2 + 2B_{22}^2)}{5}} = \sqrt{\frac{\pi(2 + \alpha^2)}{0.3}}\Delta E_{MAX}(^7F_1),$$

$$(2)$$

where α is given by

$$\alpha = \frac{E_b - E_c}{\Delta E_{MAX}/2} \qquad\qquad (3)$$

and E_b is the barycenter of energy of the $^7F_1$ level, calculated as the mean energy of the corresponding three Stark levels, whereas E_c is the energy of the central Stark level.

The scalar CF strength parameter calculated with the Eq. (2), considering only the second rank CF parameters 'with' and 'without J-mixing', as a function of maximum splitting of the $^7F_1$ level is shown in Fig. 4. The scalar CF strength calculated 'with J-mixing' shows a gradual deviation from the linear behavior for larger splittings showing, for a $^7F_1$ maximum splitting of 420 cm^{-1}, an increase of more than 10% compared to 'without J-mixing', which in turns is practically the same as those calculated using the Eqs. (2) and (3) developed by Malta et al. [12]. This difference gives a measure of the influ-

ence of the J-mixing effect in the crystal-field analysis and is due to the gradual increase in the mixing of the wave functions of the $^7F_1$ Stark level, especially for the highest energy one with those of $^7F_2$ Stark levels. This measurement allows to make a rough distribution between weak ($\Delta E_{MAX}(^7F_1) < 300$ cm^{-1}), medium (300 cm^{-1} < $\Delta E_{MAX}(^7F_1) < 450$ cm^{-1}) and strong ($\Delta E_{MAX}(^7F_1) > 450$ cm^{-1}) CF environments [6,18]. Analysing the line profile of the $^7F_0 \rightarrow {}^5D_0$ transition (Fig. 2), assuming an equal transition probability for all the Eu^{3+} environments, around 80% of the Eu^{3+} ions occupy weak CF environments and practically the rest of them are in medium CF ones, being residually in strong CF environments. It is worth noting that this result is quite similar to that found in fluoride glasses [4], and rather untypical in oxide glasses.

The scalar CF strength N_v, calculated from CF parameters with J-mixing, as a function of excitation wavelength to $^5D_0$ level for lead borate, lithium fluoroborate [5], calcium diborate [6] and sodium borosilicate [13] glasses are compared in Fig. 5. From the CF strength values, the local structure of Eu^{3+} ions found in lead borate glass is almost similar to calcium diborate glass but with a smaller distribution of environments and lies intermediate between sodium borosilicate and lithium fluoroborate glasses.

The lower crystal-fields and lower distribution of environments found in lead borate glass compared to other pure oxide glasses is due to the tendency of lead to form strong Pb–O bonds which decrease the CF strength and increase the symmetry around the Eu^{3+} ion [7]. This is further supported by the observation of Gang and Powell [31] that heavier modifier ions produce a greater amount of local order around the Eu^{3+} ion.

5. Conclusions

Local structural variations of the Eu^{3+} ion in lead borate glass have been investigated by analyzing its broad-band and site selective spectral properties. The variations of CF parameters with excitation energy are similar to those observed in other oxide glasses. A systematic variation in the optical properties with excitation energy suggests the existence of a unique kind of site for all the environments of Eu^{3+} ions in the lead borate glass. The Eu^{3+} ions preferentially bond with groups formed by PbO_4-bridged-BO_3 units giving rise to a more flexible local structure with high order and close in energy environments. The crystal-field acting on the Eu^{3+} ions in lead borate glass is almost similar to that of Eu^{3+}-doped calcium diborate glass, except of a much narrower distribution of environments with weak and medium CF strengths, and lies intermediate between Eu^{3+}-doped sodium borosilicate and lithium

fluoroborate glasses. Systematic crystal-field analysis indicates that for larger $^7F_1$ splittings the '*J*-mixing' effect should not be ignored.

Acknowledgement

References

[1] A.A. Kaminskii, Ann. Phys-France 16 (1991) 639.
[2] G. Blasse, B.C. Grabmaier, Luminescent Materials, Springer, Berlin, 1994.
[3] M.J. Weber, in: W.M. Yen, P.M. Selzer (Eds.), Laser Spectroscopy of Solids, Springer, Berlin, 1986, p. 189.
[4] V.D. Rodríguez, V. Lavín, U.R. Rodríguez-Mendoza, I.R. Martín, Opt. Mater. 13 (1999) 1.
[5] V. Lavín, P. Babu, C.K. Jayasankar, I.R. Martín, V.D. Rodríguez, J. Chem. Phys. 115 (2001) 10935.
[6] V. Lavín, U.R. Rodríguez-Mendoza, I.R. Martín, V.D. Rodríguez, J. Non-Cryst. Solids 319 (2003) 200.
[7] R. Rolli, G. Samoggia, M. Bettinelli, A. Speghini, M. Wachtler, J. Non-Cryst. Solids 288 (2001) 114.
[8] B.N. Meera, A.K. Sood, H. Chandrabhus, J. Ramakrishna, J. Non-Cryst. Solids 126 (1990) 224.
[9] A.-M. Zahra, C.Y. Zahra, J. Non-Cryst. Solids 155 (1993) 45.
[10] D.L. Griscom, in: Borate Glasses. Sructure, Properties and Applications, Plenum, New York, 1978, p. 11.
[11] F. Auzel, Mater. Res. Bull. 14 (1979) 223.
[12] O.L. Malta, E. Antic-Fidancev, M. Lemaitre-Blaise, A. Milicic-Tang, M. Taibi, J. Alloy. Compd. 228 (1995) 41.
[13] G. Pucker, K. Gatterer, H.P. Fritzer, M. Bettinelli, M. Ferrari, Phys. Rev. B 53 (1996) 6225.
[14] W.T. Carnall, P.R. Fields, K. Rajnak, J. Chem. Phys. 49 (1968) 4450.
[15] G. Nishimura, T. Kushida, J. Phys. Soc. Jpn. 60 (1991) 683;
G. Nishimura, T. Kushida, J. Phys. Soc. Jpn. 60 (1991) 695.
[16] P. Babu, C.K. Jayasankar, Physica B 279 (2000) 262.
[17] B.G. Wybourne, Spectroscopic Properties of Rare Earths, Wiley-Interscience, New York, 1965.
[18] C. Gorller-Walrand, K. Binnemans, in: K.A. GschneidnerJr., L. Eyring (Eds.), Handbook on the Physics and Chemistry of Rare Earths, vol. 23, North-Holland, Amsterdam, 1996, p. 121 (Chapter155).
[19] R. Rolli, G. Samoggia, A. Speghini, M. Bettinelli, M. Montagna, M. Ferrari, Mater. Res. Soc. Symp. Proc. 560 (1999) 169.
[20] P.J. Bray, M. Leventhal, H.O. Hooper, Phys. Chem. Glasses 4 (1963) 47.
[21] M. Leventhal, P.J. Bray, Phys. Chem. Glasses 6 (1965) 113.
[22] H. Kuroda, S. Shionoya, T. Kushida, J. Phys. Soc. Jpn. 33 (1972) 126.
[23] G. Blasse, D.J. Dirksen, Inorg. Chim. Acta 145 (1988) 303.
[24] L. Ambrosi, M. Bettinelli, M. Ferrari, M. Casarin, A. Piazza, J. Phys. (Paris) Colloq. 55 (1994) C4-477.
[25] A. Piazza, A. Bouajaj, M. Ferrari, M. Montagna, R. Campostrini, G. Carturan, J. Phys. (Paris) Colloq. 55 (1994) C4-569.
[26] E.I. Kamitsos, M.A. Karakassides, G.D. Chryssikos, J. Phys. Chem. 90 (1986) 4528;
E.I. Kamitsos, M.A. Karakassides, G.D. Chryssikos, J. Phys. Chem. 91 (1987) 1073.
[27] T. Iliescu, I. Ardelean, V. Simon, D. Maniu, J. Mater. Sci. Lett. 14 (1995) 393.
[28] U. Selvaraj, K.J. Rao, Spectrochim. Acta A 40 (1984) 1081.
[29] V. Lavín, I.R. Martín, U.R. Rodríguez-Mendoza, V.D. Rodríguez, J. Phys.: Condens. Matter 11 (1999) 8739.
[30] K. Fujita, K. Tanaka, K. Hirao, N. Soga, J. Appl. Phys. 81 (1997) 924.
[31] X. Gang, R.C. Powell, J. Appl. Phys. 57 (1985) 1299.